Room-Temperature Synthesis and Characterization of Nanocrystalline CdS, ZnS, and $Cd_xZn_{1-x}S$

Wenzhong Wang, Igor Germanenko, and M. Samy El-Shall*

Department of Chemistry, Virginia Commonwealth University, Richmond, Virginia 23284-2006

Received January 30, 2002. Revised Manuscript Received May 1, 2002

A novel and simple chemical reduction route at room temperature is described to synthesize nanocrystalline CdS, ZnS, and $Cd_xZn_{1-x}S$. In the method, anhydrous $CdCl_2$, or $ZnCl_2$, S, and KBH_4 powders react at room temperature in various organic solvents, and the effect of the solvent on the quality of the nanoparticle product is investigated. Among the solvents used, tetrahydrofuran is shown to produce the highest quality single-phase nanoparticles. The nanoparticles are characterized by X-ray diffraction, transmission electron microscopy, UV−vis absorption, and photoluminescence. The particle size ranges from 4 to 8 nm. In the $Cd_xZn_{1-x}S$, the lattice structure gradually changes from cubic to hexagonal with increasing percentage of Zn in the ternary compound $Cd_xZn_{1-x}S$. The nanoparticles exhibit broad emission peaks that shift to shorter wavelength with increasing percentage of Zn in the ternary compound $Cd_xZn_{1-x}S$. The control of the composition of $Cd_xZn_{1-x}S$ nanoparticles may lead to the development of ideal materials for short wavelength diode laser applications.

Introduction

The synthesis and characterization of semiconductor nanoparticles have attracted much interest because of their novel properties as a consequence of the large number of surface atoms and the three-dimensional confinement of the electrons.[1−7] Altering the size of the particles alters the degree of the confinement of the electrons and affects the electronic structure of the solid, especially the band gap edges, which are tunable with particle size. Among a variety of semiconductor materials, the binary metal chalcogenides of group II have been extensively studied.[1−20] They have outstanding potential applications, owing to their nonlinear optical and luminescence properties,[1−10] quantum size effect,[1−13] and other important physical and chemical properties.[14−20] For example, nanocrystalline thin films of CdS and ZnS are attractive materials in photoconducting cells and optoelectronic devices such as solar cells and photodetectors.[21−23] Also, the related ternary compounds $Cd_xZn_{1-x}S$ are promising materials for high-density optical recording and for blue or even ultraviolet laser diodes.[24−28] These applications are based on the quantum-well structures of $Cd_xZn_{1-x}S$, which exhibit fundamental absorption edges that can be varied from green to UV.[24] Unlike the quaternary $Mg_yZn_{1-y}S_xSe_{1-x}$ compounds where controlling the composition is a challenging requirement for attaining a lower lasing wavelength, the $Cd_xZn_{1-x}S$ composition can only be controlled by the lower vapor pressure of the cationic constituents and is thus expected to be more precise and reproducible.[24−31] These properties suggest that nanocrystalline $Cd_xZn_{1-x}S$ may be an ideal material for short wavelength laser diode applications.

* To whom correspondence should be addressed.

(1) Henglein, A. *Chem. Rev.* **1989**, *89*, 1861.
(2) Steigerwald, M. L.; Brus, L. E. *Acc. Chem. Res.* **1990**, *23*, 183.
(3) Bawendi, M. G.; Steigerwald, M. L.; Brus, L. E. *Annu. Rev. Phys. Chem.* **1990**, *41*, 477.
(4) Wang, Y.; Herron, N. *J. Phys. Chem.* **1991**, *95*, 525.
(5) Weller, H. *Adv. Mater.* **1993**, *5*, 88.
(6) Alivisatos, A. P. *Science* **1996**, *271*, 933.
(7) Eychmuller, A. *J. Phys. Chem. B* **2000**, *104*, 6514.
(8) Bawendi, M. G.; Wilson, W. L.; Rothberg, L.; Carrol, P. J.; Jedju, T. M.; Steigerwald, M. L.; Brus, L. E. *Phys. Rev. Lett.* **1990**, *65*, 1623.
(9) Bawendi, M. G.; Carroll, P. J.; Wilson, W. L.; Brus, L. E. *J. Chem. Phys.* **1992**, *96*, 1335.
(10) Hoheisel, W.; Volvin, V. L.; Johnson, C. S.; Alivisatos, A. P. *J. Chem. Phys.* **1994**, *101*, 8455.
(11) Murry, C. B.; Kagan, C. R.; Bawendi, M. G. *Science* **1995**, *270*, 1335.
(12) Rossetti, R.; Hill, R.; Gibson, J. M.; Brus, L. E. *J. Chem. Phys.* **1995**, *82*, 522.
(13) Weller, H. *Angew. Chem., Int. Ed. Engl.* **1993**, *32*, 41.
(14) Mann, S. *Nature* **1988**, *322*, 119.
(15) Murray, C. B.; Norris, D. J.; Bawendi, M. G. *J. Am. Chem.* Soc. **1993**, *115*, 8706.
(16) Brawn, P. V.; Osenar, P.; Stupp, S. I. *Nature* **1996**, *380*, 325.
(17) Greenham, N. C.; Peng, X. G.; Alivisatos, A. P. *Phys. Rev. B* **1996**, *54*, 17628.
(18) Colvin, V. L.; Schlamp, M. C.; Alivisatos, A. P. *Nature* **1994**, *370*, 354.
(19) Dabbousi, B. O.; Bawendi, M. G.; Onitsuka, O.; Rubner, M. F. *Appl. Phys. Lett.* **1995**, *66*, 1316.
(20) Gorer, S.; Ganske, J. A.; Hemminger, J. C.; Penner, R. M. *J. Am. Chem. Soc.* **1998**, *120*, 9584.
(21) Stanley, A. G. In "Cadmium Sulfide Solar Cells" *Applied Solid State Science 15*; Wolfe, R., Ed.; Academic Press: New York, 1975.
(22) Tsai, C. T.; Chuu, D. S.; Chen, G. L.; Yang, S. L. *J. Appl. Phys.* **1996**, *79*, 9105.
(23) Britt, J.; Ferekides, C. *Appl. Phys. Lett.* **1993**, *62*, 2851.
(24) Taguchi, T.; Endoh, Y.; Nozue, Y. *Appl. Phys. Lett.*, **1991**, *56*, 342.
(25) Wu, B. J.; Cheng, H.; Guha, M. A.; Haase, M. A.; De Puydt, J. M.; Meis-Haugen, G.; Qiu, J. *Appl. Phys. Lett.* **1993**, *63*, 2935
(26) Guha, S.; Wu, B. J.; Cheng, H.; Depuydt, J. M. *Appl. Phys. Lett.* **1993**, *63*, 2129
(27) Haase, M. A.; Qiu, J.; DePuydt, J. M.; Cheng, H. *Appl. Phys. Lett.* **1991**, *59*, 1272.
(28) Jeon, H.; Ding, J.; Patterson, W.; Nurmikko, A. V.; Xie, Grillo, D. C.; Kobayashi, M.; Gunshor, R. L. *Appl. Phys. Lett.* **1991**, *59*, 3619.
(29) Yamaga, S.; Yoshikawa, A. *J. Cryst. Growth* **1992**, *117*, 353.
(30) Sebastian, P. J.; Narvaez, J. *Thin Solid Films* **1996**, *287*, 130.
(31) Yamajuchi, T.; Yamamoto, Y.; Tanaka, T.; Yoshida, A. *Thin Solid Films* **1999**, *343*, 516.

10.1021/cm020040x CCC: $22.00
Published on Web 06/08/2002

To date, various methods have been developed to synthesize nanoparticles of Group II−VI semiconductors. Conventionally, ionic reactions in liquids ,[4,32] gas−liquid precipitation,[33] and solid-state reactions[34,35] have been utilized to prepare CdS. Other methods involve arrested precipitation from simple inorganic ions using polyphosphate[36] and low molecular weight thiols[37,38] as stabilizers. Polymers, dendrimers, and block copolymers have also been used as specific stablizers for the solution synthesis of CdS nanoparticles.[39−41] Qian and co-workers developed a solvothermal method to obtain many kinds of semiconductors including CdS.[42,43] The reactions were carried out at relatively high temperature and pressure in nonaqueous solvents using an autoclave. However, it is well-known that group II−VI materials form defects and interdiffuse at temperatures above 500 °C. Therefore, low-temperature growth of group II−VI semiconductors provides several attractive advantages.[44] Parkin and co-workers reported a liquid ammonia method for synthesizing metal chalcogenides at room temperature.[45,46] In this method, the initial solvation process should be conducted at −77 °C, and such reactions in liquid ammonia may lead to explosions. The products obtained, ZnE and CdE (E = S, Se, Te), were X-ray amorphous and crystallized above 300 °C. Recently, O'Brien used tri-*n*-octylphosphine oxide to prepare CdS nanoparticles via the thermolysis of $CdCl_2$ at 250 °C.[47] Although most of the methods developed to synthesize nanocrystalline CdS and ZnS are of widespread importance,there are some limitations to their utilities. For example, some methods require relatively high temperature for crystallization or employ toxic agents such as H_2S or require organometallic precursors that are always toxic, air, and moisture sensitive.[45−48] Recently, the room-temperature synthesis of nanocrystalline selenides has been reported.[49] The method is based on the coordination of Lewis base solvents with the metal ions where the reaction with Se^{2-} can occur at room temperature. This soft chemical route does not require organometallic precursors or the use of any complicated equipment.

In this paper, we report a novel chemical reduction route to CdS, ZnS, and $Cd_xZn_{1-x}S$ nanocrystals at room temperature. Anhydrous $CdCl_2$, or $ZnCl_2$, sulfur, and KBH_4 powders are used as reactants. The reactions are carried out in a variety of solvents, and the effect of the solvent on the product quality is investigated. The room-temperature synthesis produces high-quality nanocrystals as revealed by electron microscopy, optical, and photoluminescence measurements. We also report the photoluminescence properties of five different controlled compositions of $Cd_xZn_{1-x}S$ nanocrystals. These materials could have important applications for the development of short-wavelength optoelectronic devices.

Experimental Section

Typically, an appropriate amount of sulfur powder was added to a flask containing 50 mL of tetrahydrofuran (THF). After being stirred magnetically for 5 min, the mixture became a colorless transparent solution. A stoichiometric amount of $CdCl_2$ was added to the flask and a white suspension formed upon stirring. After the addition of KBH_4, the suspension turned light yellow. After the mixture was stirred for 12 h, a yellow precipitate formed, which was filtered and then washed with CS_2, ethanol, and distilled water in sequence several times to remove possible impurities such as KCl and excess sulfur. Then the precipitate was dried at room temperature for 12 h and collected for characterization. For the preparation of nanocrystalline ZnS, the process was the same as above except that anhydrous $ZnCl_2$ was used instead of $CdCl_2$. For the preparation of $Cd_xZn_{1-x}S$, stoichiometric anhydrous $ZnCl_2$ and $CdCl_2$ powders were used according to the molar ratios in the target compounds $Cd_{0.95}Zn_{0.05}S$, $Cd_{0.80}Zn_{0.20}S$, $Cd_{0.72}Zn_{0.28}S$, $Cd_{0.22}Zn_{0.78}S$, and $Cd_{0.10}Zn_{0.90}S$.

The X-ray powder diffraction (XRD) was obtained using a X'Pert Philips Materials Research Diffractometer using Cu $K\alpha_1$ radiation and employing a scanning speed of 0.02° s^{-1} in the 2θ range 5−75°. Electron diffraction (ED) and transmission electron microscope (TEM) images were obtained using the JEOL JEM-200FXII TEM operated at 200 kV. UV−vis absorption spectra were recorded using a Shimadzu UV-265 spectrometer with a 1-cm quartz cell at room temperature. Colloid solutions in ethanol were prepared ultrasonically for the UV−vis and the photoluminescence (PL) measurements. The PL of CdS and $Cd_xZn_{1-x}S$ nanoparticles were measured using pulsed laser excitation (355 and 266 nm, the third and fourth harmonics, respectively of a Nd:YAG laser). Dispersed PL spectra were obtained on a SPEX 1403 double-arm monochromator, detected by an RCA C31034 photomultiplier, and recorded with a computer.

Results and Discussion

Figure 1 displays the XRD patterns obtained from (a) CdS nanoparticles prepared using different solvents as indicated and (b) ZnS nanoparticles prepared using THF as a solvent. It is clear that the XRD pattern of the CdS nanoparticles exhibits prominent peaks at scattering angles (2θ) of 25, 28, 45, 48, and 53, which could be indexed to scattering from the 100, 101, 110, 103. and 112 planes, respectively, of the hexagonal CdS crystal lattice.[50] This indicates that the CdS nanoparticles have the hexagonal phase with no evidence for the incorporation of the cubic phase. In particular, the XRD peaks at 28.4 and 53 are associated only with the hexagonal

(32) Bandaranayake, K. J.; Wen, G. W.; Lin, J. Y.; Jing, H. X.; Sorensen, C. M. *Appl. Phys. Lett.* **1995**, *67*, 831.
(33) Borade, R. B. *Zeolites* **1987**, *7*, 398.
(34) Williams; R.; Yocom, P. N.; Stofko, F. S. *J. Colloid Interface Sci.* **1985**, *106*, 388.
(35) Thompson, A. H. *Mater. Res. Bull.* **1975**, *10*, 915. Coucouvanis, D. *Prog. Inorg. Chem.* **1979**, *26*, 301.
(36) Spanhel, L.; Haase, M.; Weller, H., Henglein, A. *J. Am. Chem. Soc.* **1987**, *109*, 5649.
(37) Vossmeyer, T.; Katsikas, L.; Giersig, M.; Popovic, I. G.; Diesner, K.; Chemseddine, A.; Eychmuller, A.; Weller, H. *J. Phys. Chem.* **1994**, *98*, 7665.
(38) Rockenberger, J.; Troger, L.; Kornowski, A.; Vossmeyer, T.; Eychmuller, A.; Feldhaus, J.; Weller, H. *J. Phys. Chem. B* **1997**, *101*, 2691.
(39) Sooklal, K.; Hanus, L. H.; Ploehn, H. J.; Murphy, C. J. *Adv. Mater.* **1998**, *10*, 1083.
(40) Carrot, G.; Scholz, S. M.; Plummer, C. J. G.; Hilborn, J. G.; Hedrick. J. L. *Chem. Mater.* **1999**, *11*, 3571.
(41) Huang, J.; Sooklal, K.; Murphy, C. J.; Ploehn, H. J. *Chem. Mater.* **1999**, *11*, 3595.
(42) Li, Y. D.; Liao, H. W.; Ding, Y.; Fan, Y.; Zhang, Y.; Qian, Y. T. *Inorg. Chem.* **1999**, *38*, 1382.
(43) Yu, S. H.; Yang, J.; Han, Z. H.; Zhou, Y.; Yang, R. Y.; Qian, Y. T.; Zhang, Y. *J. Mater. Chem.* **1999**, *9*, 1283.
(44) Jones, A. C. *Chem. Soc. Rev.* **1997**, 101.
(45) Henshaw, G.; Parkin, P.; Shaw, G. *Chem. Commun.* **1996**, 1095.
(46) Henshhaw, G.; Parkin, P.; Shaw, G. *J. Mater. Sci. Lett.* **1996**, *15*, 1741.
(47) Lazell, M.; O'Brien, P. *J. Mater. Chem.* **1999**, *9*, 1381.
(48) Routkevitch, D.; Bigioni, T.; Moskovits, M.; Xu, J. M. *J Phys. Chem.* **1996**, *100*, 14037.
(49) Wang, W.; Geng, Y.; Yan, P.; Liu, F.; Xie, Y.; Qian, Y. *J. Am. Chem. Soc.* **1999**, *121*, 4062.
(50) JCPDS File No. 2-549.

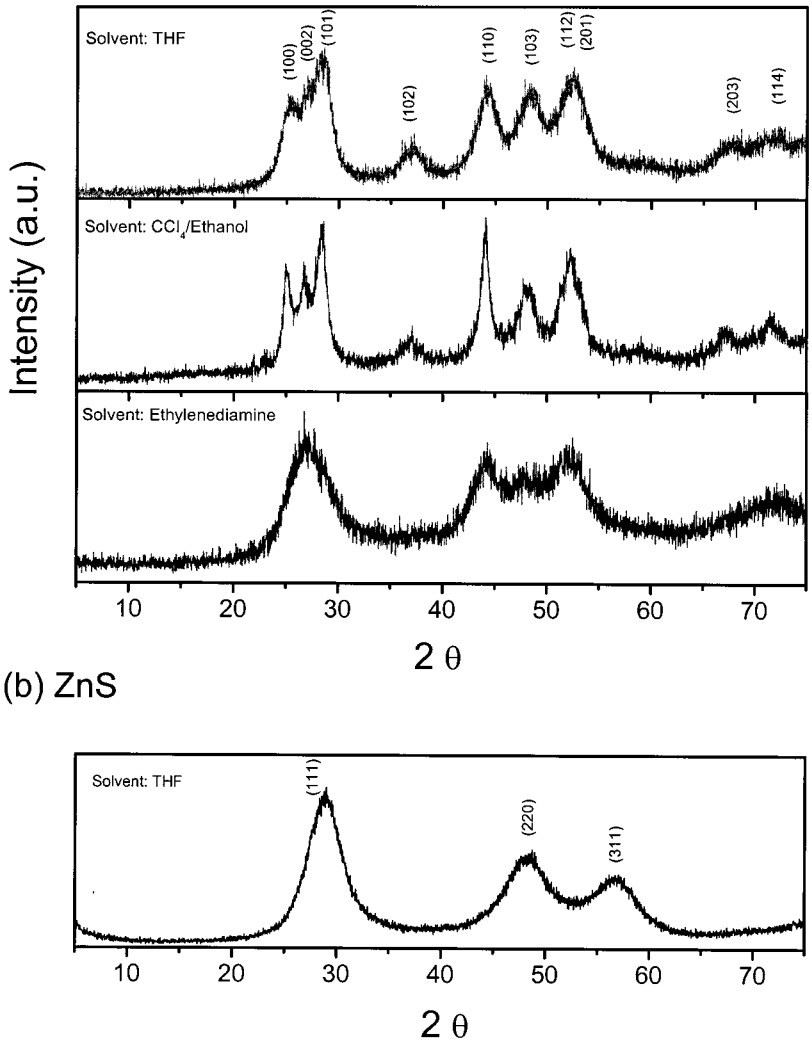

Figure 1. XRD patterns of the prepared (a) CdS and (b) ZnS nanocrystals in different solvents.

phase. The absence of the peak at 31.5 also provides good evidence for the absence of the cubic phase. The unit cell constants $a = 4.161$ Å and $c = 6.698$ Å, calculated from the XRD pattern of CdS nanoparticles shown in Figure 1a, are in good agreement with the reported values of bulk CdS with a wurtzite structure ($a = 4.142$ Å and $c = 6.724$ Å).[50] From the half-width of the XRD peaks, the average particle size is estimated as 5 nm, based on the Scherrer equation ($D = 0.9\lambda/B \cos\theta$, where D is the crystal diameter, λ is the X-ray wavelength 1.5408 Å, and θ is the diffraction angle).[42]

The XRD pattern of the as-prepared ZnS nanocrystals using THF as a solvent is shown in Figure 1b. The pattern matches well with the reference XRD of bulk ZnS.[51] The cell constant $a = 5.34$ Å, calculated from the XRD of the ZnS nanoparticles, is also in good agreement with the reported value of cubic ZnS ($a = 5.345$ Å).[51]

Different Lewis base solvents were examined to study the effect of solvent on the quality of the CdS nanoparticles. Both sulfur and anhydrous $CdCl_2$ powders dissolve completely in THF, ethylenediamine, and pyridine after magnetic stirring for 5 min. A mixed solvent of 30% ethanol and 70% CCl_4 was also used because anhydrous $CdCl_2$ powder could not be dissolved in pure CCl_4. The XRD patterns of as-prepared CdS nanoparticles showed that the samples obtained from THF, ethylenediamine, and a CCl_4/ethanol mixture match well with the XRD pattern of bulk CdS. The use of ethylenediamine as a solvent results in a smaller grain size of the CdS nanoparticles as indicated by the width of the diffraction peaks based on the Scherrer equation. As a result of the extensive peak broadening, the XRD pattern of CdS nanoparticles prepared in ethylenediamine shows the merging of the (100), (002), and (101) diffraction peaks into one broad peak and the disappearance of the (102), (203), and (114) diffraction peaks as shown in Figure 1a. The XRD of the product obtained using pyridine as a solvent (not shown) is relatively complicated and does not match well with the reference pattern of CdS. Possibly the final product is a complex of Cd and S with pyridine. There is also evidence for the presence of a small amount of sulfur in the final product.

The solvent effect observed in the preparation of ZnS nanoparticles was similar to the trend observed with CdS, thus suggesting that the role played by the solvent is the same in the preparation of CdS and ZnS nanoparticles.

From the above, we conclude that the selection of the solvent is a key factor for obtaining high-quality CdS and ZnS nanocrystals via the room-temperature reduction route. The reactions between $CdCl_2$ or $ZnCl_2$ and

(51) JCPDS File No. 80-20.

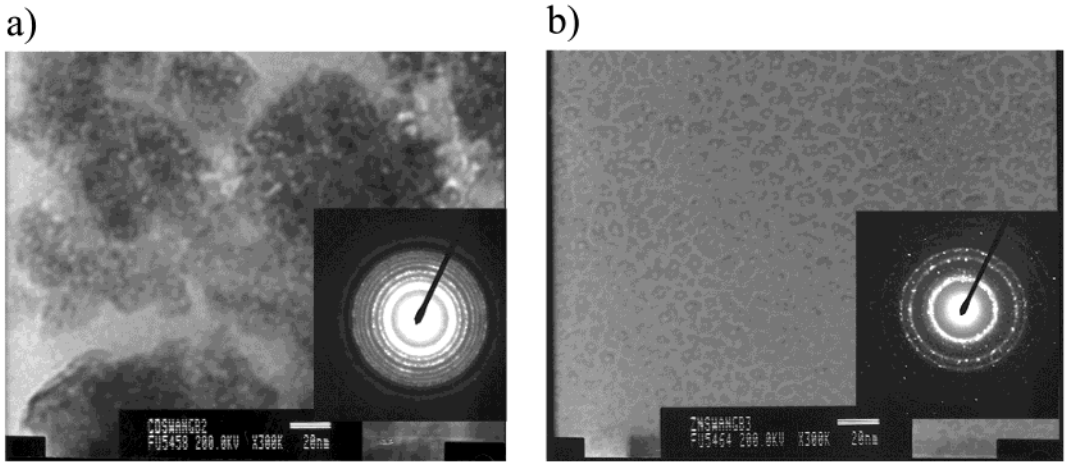

Figure 2. TEM images and ED patterns of (a) CdS and (b) ZnS nanocrystals prepared using THF as a solvent.

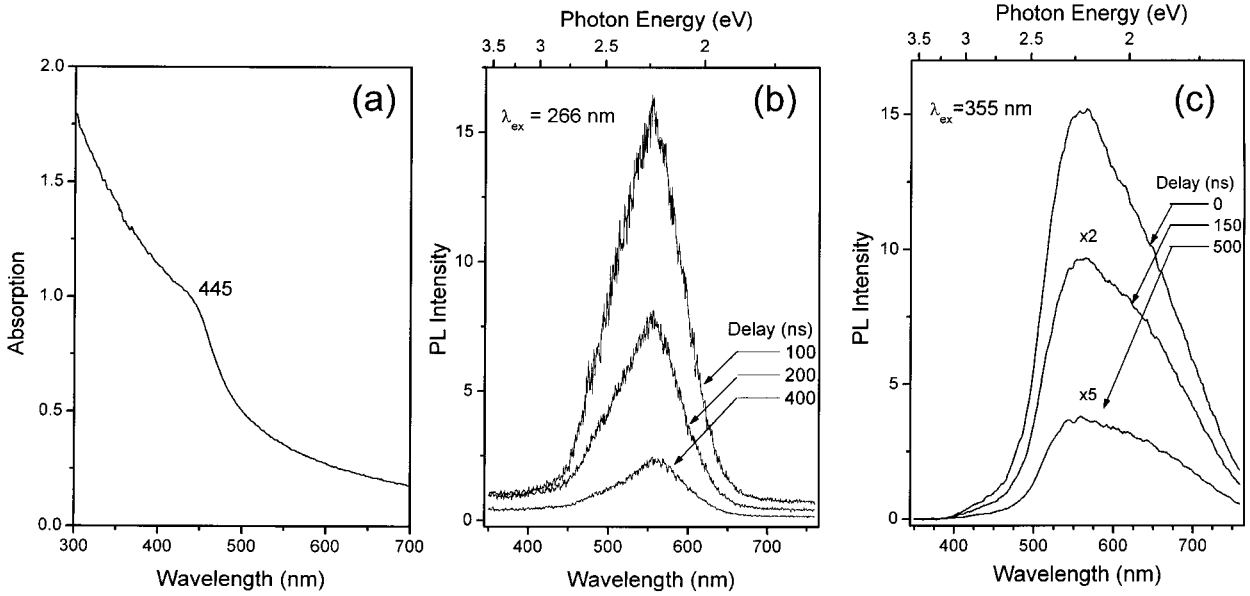

Figure 3. (a) UV−vis absorption spectrum of CdS nanocrystals. Photoluminescence spectra of CdS nanocrystals measured at different delays with respect to the laser excitation pulse of (b) 266 and (c) 355 nm.

S can be initiated at room temperature only in homogeneous solutions by using the appropriate solvent. Some mixed solvents such as CCl_4/ethanol allow the reactions to take place homogeneously. The role of KBH_4 is to reduce S to S^{2-} first so that S^{2-} can then react with Cd^{2+} or Zn^{2+} to form CdS or ZnS, respectively, at room temperature. The critical role played by the solvent appears to be the complex formation with Cd^{2+} or Zn^{2+}, which prevents the reduction of the metal ions by KBH_4.

The TEM images of the as-prepared CdS and ZnS nanoparticles are presented in parts a and b of Figure 2, respectively, along with the corresponding electron diffraction (ED) patterns. The CdS nanoparticles appear aggregated with an average particle size of about 4−5 nm. On the other hand, the TEM image of the ZnS nanoparticles (Figure 2b) shows much less agglomerated particles with an average size of about 4−6 nm. EDAX results confirmed that the CdS and ZnS nanoparticles are composed of Cd/S and Zn/S, respectively.

Figure 3 displays the absorption and PL spectra of the CdS nanoparticles. As shown in Figure 3a, the nanoparticles exhibit a well-defined absorption feature at 445 nm, which is considerably blue-shifted relative to the bulk band gap for hexagonal CdS crystals (515 nm), indicating quantum size effect.[1,36] The PL spectrum obtained upon the 266- and 355-nm pulsed laser excitations are shown in parts b and c of Figure 3, respectively. The spectra differ by the position of the boxcar gate, which ranges from 0- to 500-ns delay with respect to the laser excitation pulse. As the boxcar delay increases, the PL intensity decreases depending on the lifetime and decay profile of the PL. The observed broad PL peak centered between 556 and 560 nm is commonly attributed to the recombination of the charge carriers within surface states. The 355-nm excitation results in PL spectra with significant peak broadening at longer wavelengths. This is probably due to the excitation CdS nanoparticles with different particle sizes where the larger particles emit more to the red. On the other hand, the 266-nm excitation selects the smaller particles, which emit at shorter wavelengths. Further experiments to obtain narrower size distributions of the CdS nanoparticles are currently in progress. The narrow size distribution is expected to result in narrow PL peaks with improved efficiency. The PL decay results in a short lifetime (nanosecond range), which could not be

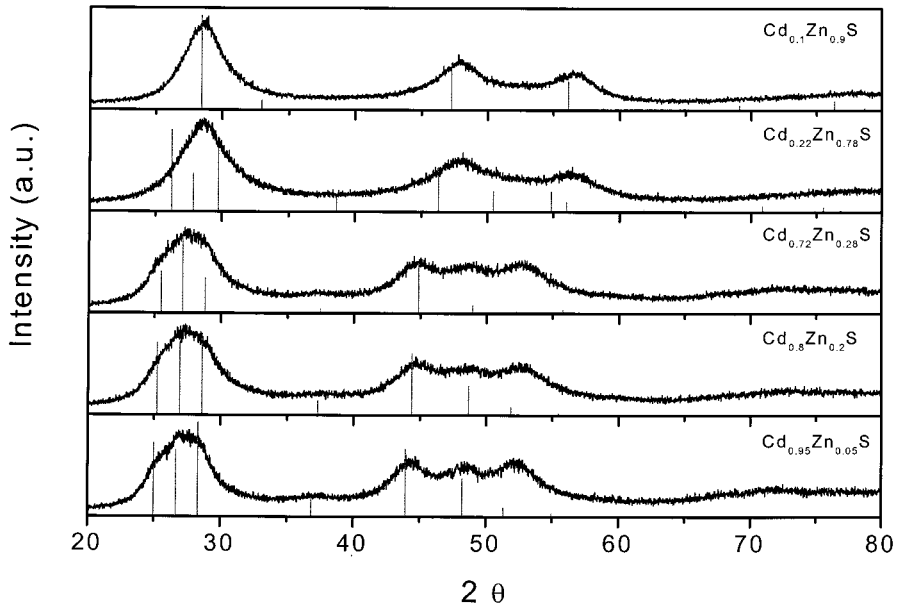

Figure 4. XRD patterns of the prepared $Cd_xZn_{1-x}S$.

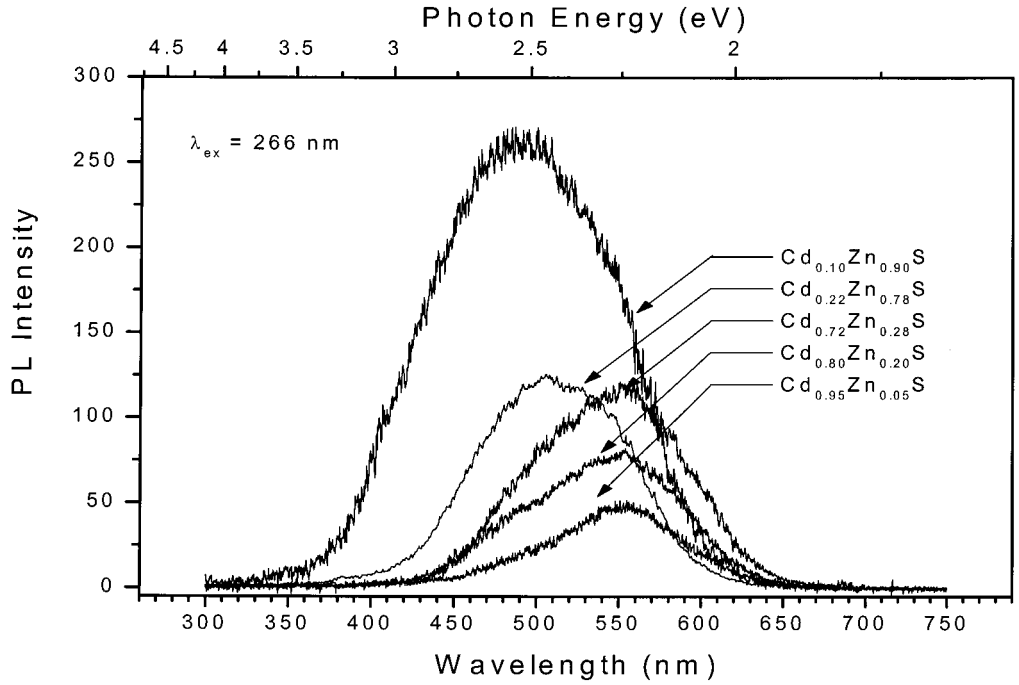

Figure 5. Photoluminescence spectra of $Cd_xZn_{1-x}S$ nanocrystals upon 266-nm excitation.

Table 1. Comparison of the Lattice Parameters of the Prepared $Cd_xZn_{1-x}S$ Nanoparticles with the Corresponding Bulk Materials

composition	calculated parameters	reference parameters	JCPDS file no.
$Cd_{0.95}Zn_{0.05}S$	hexagonal, $a = 4.11$ Å, $c = 6.70$ Å	hexagonal, $a = 4.112$ Å, $c = 6.686$ Å	40-834
$Cd_{0.80}Zn_{0.20}S$	hexagonal, $a = 4.05$ Å, $c = 6.62$ Å	hexagonal, $a = 4.069$ Å, $c = 6.621$ Å	40-835
$Cd_{0.72}Zn_{0.28}S$	hexagonal, $a = 4.06$ Å, $c = 6.63$ Å	hexagonal, $a = 4.04$ Å, $c = 6.588$ Å	40-836
$Cd_{0.22}Zn_{0.78}S$	hexagonal, $a = 3.93$ Å, $c = 6.52$ Å	hexagonal, $a = 3.92$ Å, $c = 6.405$ Å	35-1469
$Cd_{0.10}Zn_{0.90}S$	cubic, a=5.38 Å	cubic, $a = 5.43$ Å	24-1137

measured reliably using our nanosecond laser system.

Figure 4 displays the XRD patterns obtained from the $Cd_{0.95}Zn_{0.05}S$, $Cd_{0.80}Zn_{0.20}S$, $Cd_{0.72}Zn_{0.28}S$, $Cd_{0.22}Zn_{0.78}S$, and $Cd_{0.10}Zn_{0.90}S$ nanoparticles prepared using THF as a solvent. Broad XRD peaks are attributed to the absence of long-range order in these samples and reflect the small particle size (less than 4 nm as estimated from the Scherrer equation). The vertical lines displayed in each pattern represent the peak positions of the corresponding bulk material with the same composition as

the nanoparticles. It is clear that the prepared $Cd_xZn_{1-x}S$, nanoparticles have the same crystal structures as the corresponding bulk materials.

In a comparison of the XRD patterns of the five prepared $Cd_xZn_{1-x}S$ nanoparticles, it is clear that, at lower Cd:Zn ratio, as in $Cd_{0.1}Zn_{0.9}S$, the crystal structure is similar to that of the cubic ZnS lattice. On the other hand, at higher Cd:Zn ratio, as in $Cd_{0.95}Zn_{0.05}S$, the crystal structure becomes similar to that of the hexagonal CdS. It is also interesting to note that the diffraction peaks in $Cd_xZn_{1-x}S$ gradually shift to lower 2θ values (compared to the CdS pattern) as the percentage of Cd increases in material. These changes indicate that lattice structure of $Cd_xZn_{1-x}S$ changes from hexagonal to cubic as x goes from $1 \rightarrow 0$. The lattice parameters of the prepared nanoparticles compare well with the reference bulk data as shown in Table 1.

The above results reveal that we successfully obtained cadmium zinc sulfide nanoparticles at room temperature and that the compositions have been controlled. To our knowledge, there is no report that nanoparticles of the five phases, $Cd_{0.95}Zn_{0.05}S$, $Cd_{0.80}Zn_{0.20}S$, $Cd_{0.72}Zn_{0.28}S$, $Cd_{0.22}Zn_{0.78}S$, and $Cd_{0.10}Zn_{0.90}S$, have been prepared. In our experiments, by changing the ratio of $ZnCl_2$:$CdCl_2$ in the reactants, we only obtain the above five phases, and no other $Cd_xZn_{1-x}S$ phases with flexible x values are obtained.

Figure 5 displays the PL spectra of $Cd_xZn_{1-x}S$ nanoparticles following the 266-nm pulsed laser excitation. The PL emission was collected with a wide gate of 5 μs following the excitation pulse, and therefore, it represents the steady-state PL. The center of the emission peak shifts from 480, 505, 540, and 543 to 550 nm for $Cd_{0.10}Zn_{0.90}S$, $Cd_{0.22}Zn_{0.78}S$, $Cd_{0.72}Zn_{0.28}S$, $Cd_{0.80}Zn_{0.20}S$, and $Cd_{0.95}Zn_{0.05}S$, respectively.

In conclusion, well-defined compositions of nanocrystalline CdS, ZnS, and $Cd_xZn_{1-x}S$ have been prepared by a novel and simple chemical reduction route at room temperature. The control of the composition of $Cd_xZn_{1-x}S$ nanoparticles may lead to the development of ideal materials for the short wavelength diode laser applications.

Acknowledgment. The authors gratefully acknowledge support from the NASA microgravity Materials Science Program (Grant No. NAG8-1484).

CM020040X